

Cell Fate and Differentiation of the Developing Ocular Lens

Teri M. S. Greiling,¹ Masamoto Aose,¹ and John I. Clark^{1,2}

PURPOSE. Even though zebrafish development does not include the formation of a lens vesicle, the authors' hypothesis is that the processes of cell differentiation are similar in zebrafish and mammals and determine cell fates in the lens.

METHODS. Two-photon live embryo imaging was used to follow individual fluorescently labeled cells in real-time from the placode stage at 16 hours postfertilization (hpf) until obvious morphologic differentiation into epithelium or fiber cells had occurred at approximately 28 hpf. Immunohistochemistry was used to label proliferating, differentiating, and apoptotic cells.

RESULTS. Similar to the mammal, cells in the teleost peripheral lens placode migrated to the anterior lens mass and differentiated into an anterior epithelium. Cells in the central lens placode migrated to the posterior lens mass and differentiated into primary fiber cells. Anterior and posterior polarization in the zebrafish lens mass was similar to mammalian lens vesicle polarization. Primary fiber cell differentiation was apparent at approximately 21 hpf, before separation of the lens from the surface ectoderm, as evidenced by cell elongation, exit from the cell cycle, and expression of ZI-1, a marker for fiber differentiation. TUNEL labeling demonstrated that apoptosis was not a primary mechanism for lens separation from the surface ectoderm.

CONCLUSIONS. Despite the absence of a lens vesicle in the zebrafish embryo, lens organogenesis appears to be well conserved among vertebrates. Results using three-dimensional live embryo imaging of zebrafish development showed minimal differences and strong similarities in the fate of cells in the zebrafish and mammalian lens placode. (*Invest Ophthalmol Vis Sci.* 2010;51:1540-1546) DOI:10.1167/iovs.09-4388

The generation of a highly symmetric, refractile, transparent lens from a sheet of undifferentiated cranial epithelial cells is one of the most remarkable processes in development. Highly coordinated cellular proliferation, polarization, migration, and elongation lead to the reorganization of the surface cells in the lens placode to a functional optical element in the visual pathway, the ocular lens. The symmetry necessary for refraction of light and image formation in the visual system requires a high degree of precision in specifying the fates of individual cells and their spatial relationships in the adult lens. A functional visual system is especially important for species such as humans and zebrafish, in which vision is the primary sensory pathway for seeking food. Developmental defects in

the lens are extremely rare, suggestive of unique intersecting, developmental pathways that are protected against the deleterious effects of cell and molecular aging.

In mammalian, avian, and teleost species, lens formation begins as cells of the surface ectoderm become columnar to create the lens placode overlying the optic primordium in the embryonic head.¹⁻⁵ The placode invaginates to form a lens pit that deepens and pinches off from the surrounding surface ectoderm as a hollow, fluid-filled vesicle in mammalian and avian lenses. Differentiation continues based on a spatial polarization of the lens vesicle: cells in the anterior hemisphere of the lens vesicle form the anterior epithelium, and cells in the posterior hemisphere elongate and differentiate as primary fiber cells to obliterate the vesicle space. Polarization of the vesicle and cellular differentiation are thought to be influenced by extrinsic transcription and growth factors from the aqueous and vitreous humors such as FGF, IGF-1, insulin, and TGF β .⁶⁻⁸

In contrast to mammals or avians, the earliest stages of lens development in zebrafish occur without the formation of a lens vesicle.⁹⁻¹² Although described as a major difference between mammalian and teleost development, our hypothesis is that the processes of cell differentiation that determine cell fates in lens are similar in zebrafish and mammalian development. However, in the absence of a vesicle stage, the expected correspondence between cells in the anterior vesicle and the lens epithelium and the posterior vesicle and the primary fibers did not exist. Previous work using live-cell imaging demonstrated that cells in the zebrafish placode thickened and underwent progressive delamination that resembled epithelial-to-mesenchymal transition.¹ During delamination, the solid, multilayered lens cell mass was reorganized into a spherical structure that underwent cell differentiation to form an anterior epithelium and posterior elongating primary fibers, similar to the mammalian lens.^{1,12} To determine the fates of cells in the developing zebrafish lens, live-cell imaging combined with immunohistochemistry can be used to define how and when zebrafish primary fiber cells differentiate during lens development.

In this report, two-photon live-embryo imaging was used to follow individual fluorescently labeled cells in real-time to develop a fate map of the zebrafish lens placode. Cells were followed from the placode stage at 16 hours postfertilization (hpf) until obvious morphologic differentiation into epithelium or fiber cells had occurred by approximately 28 hpf. We determined that cells destined to become epithelial or primary fiber cells followed a predictable but separate path of migration during development. Cells in the peripheral lens placode migrated to the anterior lens mass and differentiated into anterior epithelium. Cells in the central lens placode migrated to the posterior lens mass and differentiated into primary fiber cells. Although a living fate map of the mammalian lens placode has never been constructed, results in the zebrafish confirm the widely accepted mammalian model: cells in the placode periphery become epithelium, and cells in the central placode become primary fibers. Immunohistochemistry demonstrated that stages of proliferation were similar to those of the mammal and that apoptosis was not a primary mechanism

From the Departments of ¹Biological Structure and ²Ophthalmology, University of Washington, Seattle, Washington.

Supported by National Eye Institute Grants EY04542 (JIC) and EY07031 (TMG).

Submitted for publication July 28, 2009; revised August 13, 2009; accepted August 13, 2009.

Disclosure: T.M.S. Greiling, None; M. Aose, None; J.I. Clark, None

Corresponding author: John I. Clark, Departments of Biological Structure and Ophthalmology, University of Washington, Box 357420, Seattle, WA 98195-7420; clarkji@u.washington.edu.

in delamination. We conclude that despite the lack of a zebrafish lens vesicle, eye organogenesis appears to be well conserved among vertebrates.

METHODS

Cell Labeling

Two-photon imaging was performed using the Q01 transgenic fish line, provided by the laboratory of Rachel O. L. Wong (Department of Biological Structure, University of Washington, Seattle, WA). Q01 fish express cyan fluorescent protein fused to a membrane-targeting sequence of zebrafish Gap43 (mCFP), driven by an EF1 α promoter and a hexamer of the DF4 pax6 enhancer element.¹³ Q01 fish were generated in a wild-type background and develop and reproduce normally. Adult fish were housed at 28.5°C. All experiments were approved by the University of Washington Institutional Animal Care and Use Committee and were conducted in compliance with the ARVO Statement for the Use of Animals in Ophthalmic and Visual Research.

Fertilized zebrafish eggs were injected at the one-cell stage with a combination of two plasmids, EF1 α ::Gal4VP16 containing a Pax6 enhancer and UAS::td-tomato, for mosaic expression of cytoplasmic fluorescent tomato red protein. Embryos with one to four tomato-labeled cells in the peripheral or central lens placode at 16 to 20 hpf were selected for two-photon time-lapse imaging every 30 to 60 minutes for up to 20 hours. Embryos with labeled cells in the midlateral region of the placode were not selected for time-lapse imaging because no clear morphologic boundary was present between the central and peripheral regions of the placode.

BrdU Injections

Zebrafish embryos aged 16 to 72 hpf were anesthetized in 0.08 mM tricaine, manually dechorionated, and injected into the yolk with 10 mM bromodeoxyuridine and 1% phenol red dissolved in 1 \times Danieau's at selected stages of development from 16 to 75 hpf. Six to 12 embryos were examined at each time point. Embryos were returned to 28.5°C for 1 to 3 hours and then were euthanatized in 0.40 mM tricaine and stained to detect proliferating cells as below. These experiments were repeated in both WIK wild-type and Q01 transgenic mCFP-labeled embryos (used for live imaging); no differences were observed between the two strains.

Imaging

Embryos were prepared for *in vivo* imaging, as described previously for retinal imaging.^{14,15} Briefly, embryos were spawned and placed in Danieau's embryo medium (17.4 mM NaCl, 0.21 mM KCl, 0.12 mM MgSO₄, 0.18 mM Ca(NO₃)₂ · 4 H₂O, 1.5 mM HEPES, pH 7.6) at 22°C to 28.5°C. Embryos were transferred to 0.2 mM 1-phenyl-2-thiourea (PTU) in Danieau's at 10 to 18 hpf to prevent melanophore development in the eye. Before imaging, embryos were anesthetized in 0.08 mM tricaine, manually dechorionated with forceps, and mounted in a Petri dish in 0.5% low melting point agarose dissolved in Danieau's, 0.2 mM PTU, and 0.08 mM tricaine. Embryos were maintained in agarose with a layer of Danieau's, 0.2 mM PTU, and 0.08 mM tricaine floating on top at 28.5°C for up to 8 hours or were released from agarose and remounted for multiple imaging sessions.

Imaging was performed on an Olympus (Tokyo, Japan) multiphoton microscope with a long working distance (25 \times ; 1.05 NA) water immersion lens. Stacks of images through the lens were taken with Olympus software (Fluoview version 1.7a) and were saved as multi-tiff files. Image stacks were further analyzed (Amira 4.1.1; Visage Imaging, Andover, MA). Digital space filling of tomato red-labeled cells was used to visualize the 3D orientation of individual differentiating cells during time-lapse cell imaging (Movie S1, <http://www.iovs.org/cgi/content/full/51/3/1540/DC1>).

Immunohistochemistry

WIK wild-type or Q01 embryos were euthanatized in 0.40 mM tricaine and fixed in 4% paraformaldehyde/5% sucrose/phosphate-buffered saline

(PBS) for 3 hours at room temperature, followed by three washes in 5% sucrose/PBS. Embryos were mounted in 1.5% low-melting point agarose/5% sucrose/PBS, and the hardened agarose block was cryoprotected in 30% sucrose/PBS overnight at 4°C. Agarose blocks were immersed in a 1:1 mixture of 30% sucrose/PBS and optimum temperature cutting compound (OCT; Tissue Tek; Sakura-Finetek, Torrance, CA) for 10 hours, followed by immersion in 100% OCT overnight. OCT blocks were frozen in liquid nitrogen and stored at -80°C. Blocks were cut in 10- μ m sections at -18°C and were mounted on charged slides.

For antibody staining, slides were blocked for 1 hour in a 1:1 mixture of 3% bovine serum albumin (BSA) and 3% fetal calf serum albumin (FSA) in PBS, followed by 2 hours in mouse primary antibody (Zl-1; ZIRC, Eugene, OR) diluted in BSA/FSA/PBS. Slides were washed and treated for 90 minutes with Alexa Fluor goat anti-mouse 488 (Molecular Probes, Eugene, OR) in BSA/FSA/PBS followed by washing in PBS. Cell membranes were counterstained with Alexa Fluor 550-conjugated wheat germ agglutinin (Molecular Probes) and sections were mounted in medium with DAPI (Vectashield; Vector Laboratories, Burlingame, CA). The antigen for Zl-1 is unknown, though Zl-1 antibody is fiber cell specific and is thought to stain a gamma crystallin (Wistow G, personal communication, 2009).¹⁶

Terminal deoxynucleotidyl transferase (TdT)-mediated dUTP nick-end labeling (TUNEL) for the detection of apoptosis was performed as described by the manufacturer (catalog no. TA4629; R&D Systems, Minneapolis, MN) except the TUNEL reaction mixture was diluted 1:1 with 30 mM Tris, pH 7.2, containing 140 mM sodium cacodylate and 1 mM CoCl₂ as described previously.¹⁷ After the final fluorescein detection step, slides were refixed for 15 minutes in 4% paraformaldehyde, washed in PBS, and treated with 0.2 U/ μ L DNase (Fermentas Life Sciences, Burlington, ON, Canada) for 15 minutes at 37°C. Slides were washed and incubated with 1:1000 mouse IgG anti-BrdU antibody (BD Biosciences)/1% BSA/0.1% gelatin/0.3% Tx-100/PBS for 2 hours at room temperature followed by 1:200 secondary Alexa Fluor goat-anti-mouse-568 antibody (Molecular Probes)/1% BSA/0.1% gelatin/PBS for 60 minutes at room temperature. Slides were finally washed in PBS and mounted in medium (Vectashield; Vector Laboratories) with DAPI.

RESULTS

Lens Placode Fate Map

In all embryos examined, cell fate (epithelium vs. primary fiber cell) could be predicted by cell position in the lens placode or lens mass. Three cells were followed in the developing lens of a living zebrafish embryo in real time from 16.5 hpf to 30 hpf (Figs. 1A-H). In the 16.5 hpf embryo, a single layer of columnar lens placodal cells in the cephalic surface ectoderm closely apposed the optic cup of the developing retina, an outgrowth of the developing diencephalon. Three cells expressing tomato red fluorescent protein in the lens placode were digitally pseudocolored blue, green, and violet, respectively. The columnar violet cell was located near the center of the lens placode at 16.5 hpf and progressively moved to the posterior lens mass from 18 to 21 hpf (Figs. 1B-E). By 25 hpf the violet cell elongated, and at 27 hpf the violet cell became a crescent-shaped primary fiber cell wrapping around the embryonic lens nucleus. At 30 hpf (Fig. 1H), the crescent-shaped violet primary fiber cell appeared to have detached from the posterior lens capsule, as additional fiber cells grew and elongated to form new layers of cells outside the violet cell. The migration and elongation of the pseudocolored orange and blue cells that started in the center of the lens placode at 16.5 hpf were similar to the migration and elongation of the purple cell (Fig. 1A'). By 17.5 hpf (Fig. 1B'), the orange cell appeared to have replicated because two fluorescent cells—now orange and green—were close together. These three cells—orange, green, and blue—moved to the posterior lens mass at 19 hpf (Fig. 1C') and began to elongate as primary fibers by 21.5 hpf and 23 hpf

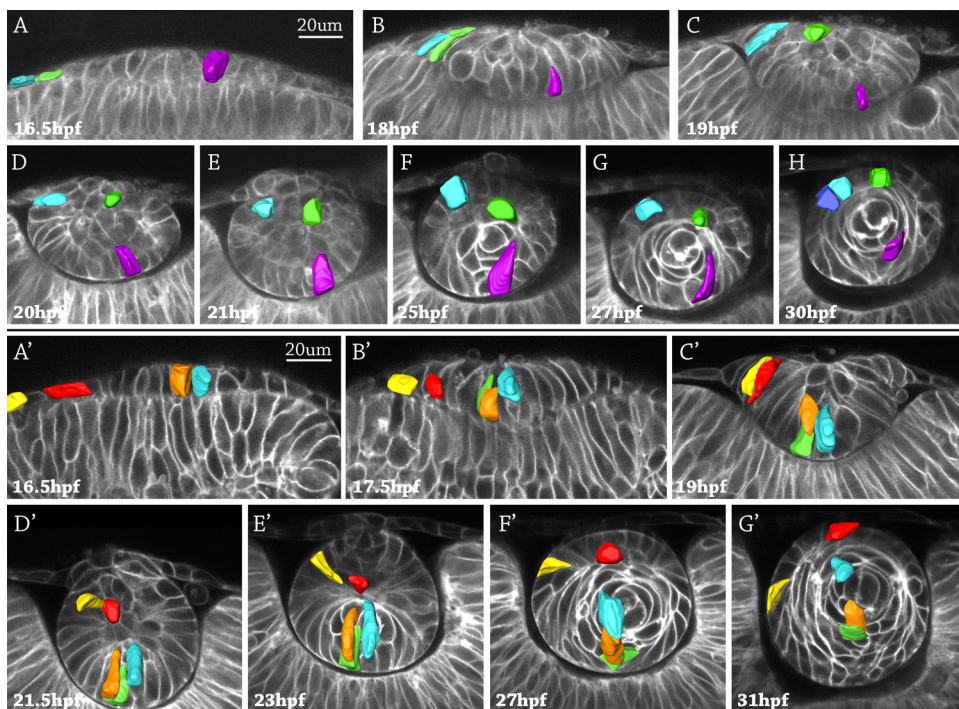


FIGURE 1. Cell fate tracking during lens development in two representative zebrafish embryos. Image stacks were acquired every 30 minutes, and representative images are shown. The surface ectoderm is oriented at the *top* of each image, and the retina is at the *bottom*. Three pseudocolored cells were followed from the lens placode stage at 16.5 hpf to obvious lens differentiation into an anterior epithelium and fiber cells at 30 hpf (A-H). Five pseudocolored cells in a different embryo were followed from 16.5 hpf to 31 hpf (A'-G'). The *violet* cell (A-H) and the *orange* and *blue* cells in (A'-G') started in the central placode, moved to the posterior lens mass (where the *orange* cell divided into two cells, *orange* and *green*), and elongated as primary fibers in the embryonic lens nucleus. The *blue* and *green* cells (A-H) and the *red* and *yellow* cells (A'-G') originated in the peripheral placode, migrated to the anterior lens mass, and became part of the anterior epithelium.

(Figs. 1D', 1E'). By 31 hpf (Fig. 1G'), the orange, green, and blue cells elongated to form a layer of primary fibers wrapping around the embryonic lens nucleus. In summary, primary fiber cell migration and elongation followed a pattern: cells originating in the central lens placode migrated to the deep/posterior surface of the lens mass and elongated to form crescent-shaped primary fibers in the embryonic lens nucleus.

A different pattern of migration and differentiation was observed for cells at the periphery of the lens placode. These cells migrated to the anterior half of the developing lens mass and, after delamination, organized into a single layer of epithelium over the anterior surface of the lens or underwent cell death. Instead of elongating, the cells remained columnar epithelial cells. The pseudocolored blue and green cells at the periphery of the lens placode at 16.5 hpf (Fig. 1A) were located in the anterior lens mass at 20 hpf (Fig. 1D). At 25 hpf (Fig. 1F), after separation of the lens from the future cornea, the blue cell was located on the anterior surface of the lens in the position of the anterior epithelium. The blue cell remained in the anterior epithelium and appeared to have proliferated by 30 hpf (Fig. 1H). At 25 hpf and 27 hpf (Figs. 1F, G), the green cell remained deep to the anterior surface of the lens mass until 30 hpf, when the green cell was observed at the surface of the lens, directly overlying elongating primary fibers (Fig. 1H). In other embryos observed, some cells in the same region as the green cell at 25 hpf appeared to undergo apoptosis rather than contribute to the anterior epithelium (Supplementary Fig. S1B, <http://www.iovs.org/cgi/content/full/51/3/1540/DC1>). A second example of the differentiation of cells in the periphery of the placode to the anterior lens mass finishing in the anterior epithelium is illustrated by the pseudocolored red and yellow cells in Figures 1A' to 1G'.

Observing cell fates in the developing zebrafish lens suggested four distinct categories or stages, which are summarized in Figure 2. Cells in the periphery of the lens placode at 16 hpf migrated to the anterior lens mass by the 20 hpf time point (Fig. 2A) and either organized into a single layer of anterior epithelial cells by 28 hpf or underwent apoptosis (Fig. 2B). Concomitantly, cells in the center of the lens placode at 16 hpf migrated along the posterior lens mass until approximately 20 hpf (Fig. 2C), when they began elongation to form primary fiber cells in the embryonic lens

nucleus (Fig. 2D). This pattern of cell migration and elongation was observed repeatedly using 105 different cells in 20 different embryos, with no deviation from the pattern. Based on real-time imaging of live cells, we hypothesize that the fate of cells in the lens placode can be predicted by cell position: central cells migrate posteriorly and elongate to become primary fibers, whereas peripheral cells migrate anteriorly to form epithelial cells in the developing zebrafish lens.

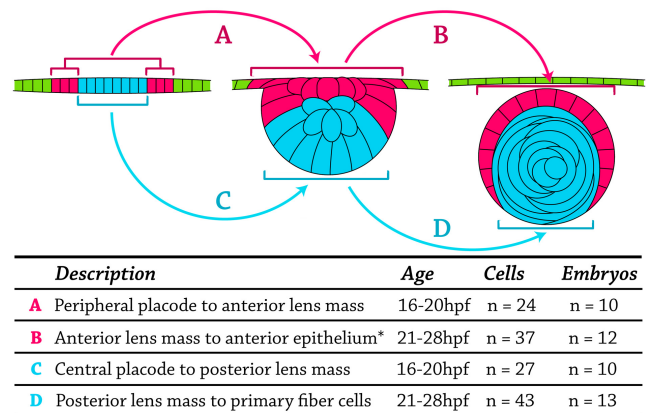


FIGURE 2. Fate-map diagram assembled from live-cell tracking experiments. *Top:* three representative stages of development are diagrammed. *Left:* lens placode at 16 hpf. Central cells (*blue*). Peripheral cells (*pink*). Cells of the surface ectoderm (not part of the placode; *green*). *Middle:* lens mass at 20 hpf. Posterior cells (*blue*). Anterior cells (*pink*). Surface ectoderm (*green*), to represent their origin outside the placode. *Right:* lens at 28 hpf. Primary fibers (*blue*). Anterior epithelium (*pink*). Cornea (*green*). (A, arrow) 24 cells in 10 embryos that moved from the peripheral lens placode to the anterior lens mass. (B, arrow) 37 cells in 12 embryos that differentiated from the anterior lens mass into the anterior lens epithelium. *Few of these cells underwent apoptosis, and they did not contribute to anterior epithelium. (C, arrow) 27 cells in 10 embryos that moved from the central lens placode to the posterior lens mass. (D, arrow) 43 cells in 13 embryos that differentiated from the posterior lens mass into primary fiber cells. No deviation from these fate map patterns was observed in all embryos studied.

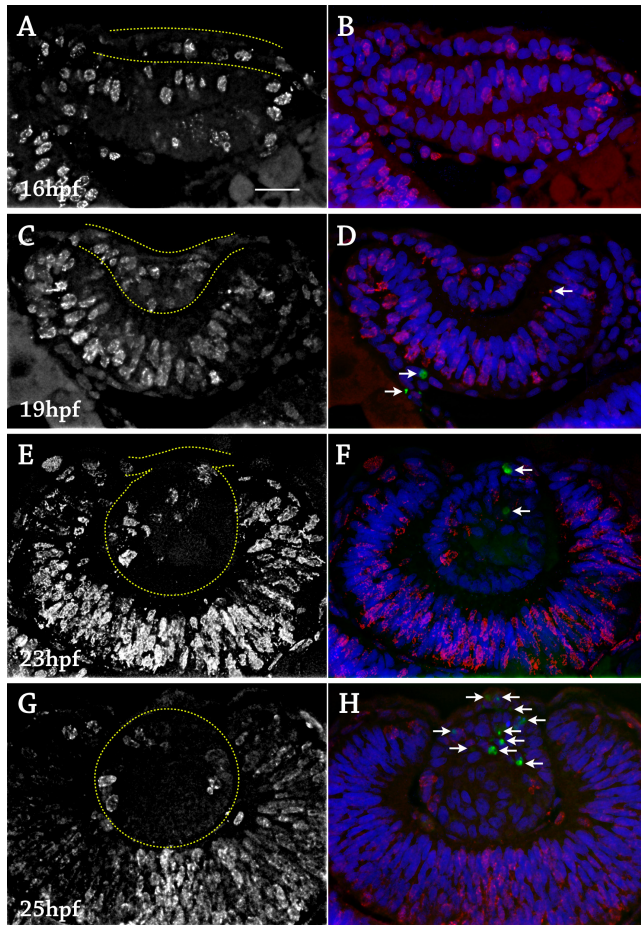


FIGURE 3. Cell birth and death in the zebrafish lens, 16 to 25 hpf. Fixed lens sections stained with anti-BrdU for proliferation (*red*), TUNEL for apoptosis (*green*, *white arrows*), and DAPI to label cell nuclei (*blue*). Six to 12 embryos were examined at each time point. (A) 16 hpf, anti-BrdU alone. The lens placode was outlined in *yellow*. Proliferation occurred throughout the placode and retina. (B) Same section as in A with DAPI and TUNEL. No apoptotic cells were detected. (C) 19 hpf, anti-BrdU alone. The lens mass was outlined in *yellow*. Proliferation occurred throughout the lens mass and retina. (D) Same section as in C with DAPI and TUNEL. A few apoptotic cells were detected in the retina (*arrows*). (E) 23 hpf, anti-BrdU alone. The delaminating lens mass was outlined in *yellow*. Proliferation was mainly in the anterior lens mass. (F) Same section as in E with DAPI and TUNEL. Two apoptotic cells were visible in the anterior lens mass (*arrows*). (G) 25 hpf, anti-BrdU alone. The lens was outlined in *yellow*. Proliferation was restricted to the lens epithelium. (H) Same section as in G with DAPI and TUNEL. Multiple apoptotic cells were detected in the anterior lens mass and cornea after separation (*arrows*). Scale bar, 20 μ m.

Cell Proliferation

In the early developing lens (16–21 hpf), BrdU-positive cells were scattered throughout the lens placode, developing lens mass, surface ectoderm, and retina, suggesting that all cells in the lens placode and lens mass were proliferative (Figs. 3A–D). At approximately 21 hpf, BrdU labeling had decreased in the posterior lens mass, suggesting that primary fiber cells exited the cell cycle as elongation began, similar to the mammalian lens. After 24 hpf, BrdU labeling was restricted to cells in the anterior lens mass that were fated to become anterior epithelium (Figs. 3A, G). By 30 hpf, BrdU-positive cells were observed only in the anterior epithelium (Figs. 4A–D). Proliferation of cells in the anterior epithelium continued until a few hours before hatching, which normally occurred by 72 hpf. At this

stage, the BrdU-positive cells were restricted to a lateral ring of cells outside the optical path that corresponded to the proliferative zone of the epithelium. Four embryos were injected with BrdU every 2 hours from 67 to 75 hpf to control for a longer cell cycle, and no cells in the central zone of the anterior epithelium were BrdU positive during this stage (Fig. 4E). In summary, three stages of proliferation were observed. In stage 1 (16–22 hpf), all cells of the lens placode and lens mass appeared to be proliferative. In stage 2 (22–67 hpf), proliferation was observed in cells of the anterior epithelium and not in the migrating, elongating fiber cells. In stage 3 (>67 hpf), proliferation was restricted to a lateral proliferative zone of the anterior epithelium outside the optical path of light.

Primary Fiber Elongation

A marker for lens fibers, Zl-1, did not stain the lens before 19 hpf (Fig. 5). At 20 hpf, one cell in the posterior lens mass was Zl-1 positive, suggesting the initiation of primary fiber differentiation. Temporally, Zl-1 labeling correlated with elongation of posterior cells observed during live-cell imaging and decreased proliferation in the posterior lens mass detected by

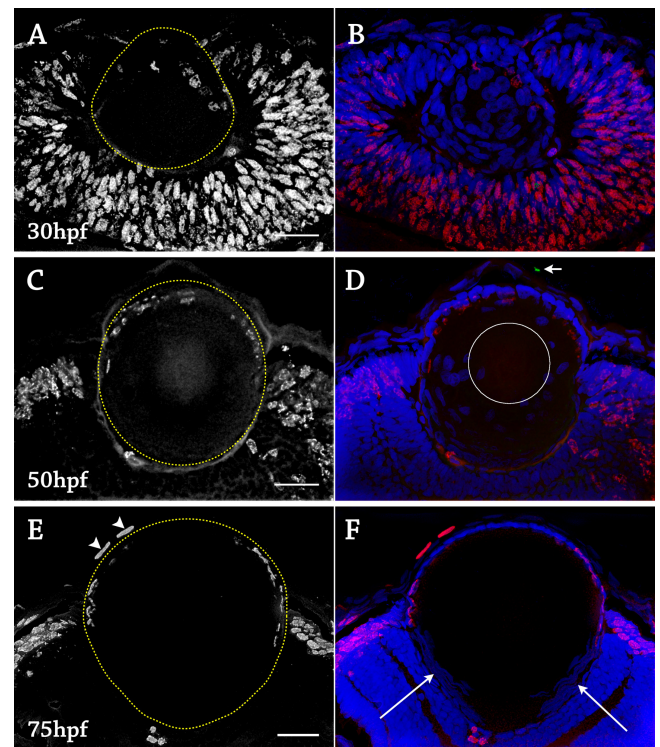


FIGURE 4. Cell birth and death in the zebrafish lens, 30 to 75 hpf. Fixed lens sections stained with anti-BrdU for proliferation (*red*), TUNEL for apoptosis (*green*), and DAPI to label cell nuclei (*blue*). Six to 12 embryos were examined at each time point. (A) 30 hpf, anti-BrdU alone. The lens was outlined in *yellow*. Proliferation was restricted to the anterior epithelium. (B) Same section as in A with DAPI and TUNEL. No apoptotic cells were detected, and all cells remained nucleated. (C) 50 hpf, anti-BrdU alone. The lens was outlined in *yellow*. Proliferation occurred throughout the anterior epithelium. (D) Same section as in C with DAPI and TUNEL. One apoptotic cell was detected in the cornea (*arrow*). Nuclei were not present in the central fibers, outlined by the *white circle*. (E) 75 hpf, anti-BrdU alone. The lens was outlined in *yellow*. Proliferation was restricted to a lateral zone. Two cells in the cornea were BrdU-positive (*arrowheads*). (F) Same section as in (E) with DAPI and TUNEL. No cells labeled with TUNEL, including maturing secondary fibers. Nuclei were present only in the anterior epithelium and the transition zone, which was located posterior to the proliferative zone (*long arrows*). Scale bars, 20 μ m.

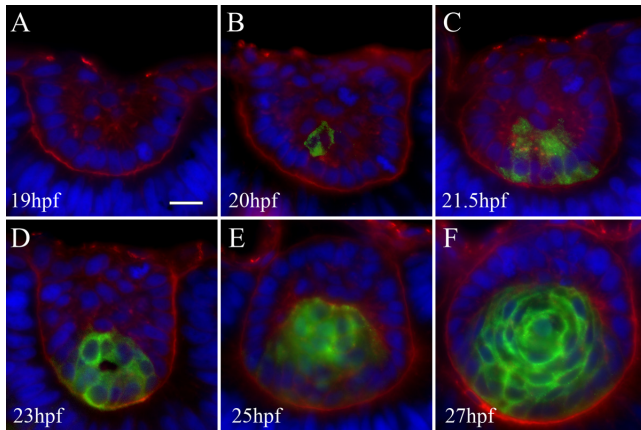


FIGURE 5. ZI-1 antibody staining primary lens fiber cells. Sections were labeled with ZI-1 (*green*), wheat germ agglutinin (*red*), DAPI (*blue*). Six to 12 embryos were examined at each time point. (A) The 19 hpf lens contained no ZI-1 staining. (B) At 20 hpf, one cell in the posterior lens mass stained with ZI-1. Primary fibers cell differentiation begins. (C, D) At 21.5 hpf and 23 hpf, increasing numbers of elongating primary fiber cells at the posterior lens mass stained with ZI-1. (E) At 25 hpf after separation of the lens and cornea, all cells in the posterior lens were ZI-1 positive, and cells in the anterior lens, which were organizing into the anterior epithelium, did not stain. (F) At 27 hpf, formation of a single layer of anterior epithelium wrapping around the lens was nearly complete. All primary fibers were ZI-1 positive.

BrdU labeling. ZI-1 labeling increased until all cells in the posterior lens mass were ZI-1 positive. At 27 hpf (Fig. 5F), all cells other than the anterior epithelium were ZI-1 positive, indicating the establishment of the embryonic lens containing primary fibers and an anterior epithelium.

Cell Death

BrdU-stained sections were also treated with TUNEL labeling to detect the double-strand DNA breaks that indicate apoptosis.^{18,19} TUNEL labeling was not observed in the lens placode or lens mass from 16 to 22 hpf (Fig. 3). Occasional TUNEL-positive nuclei were observed in the retina. From 23 to 26 hpf, TUNEL labeling was observed in the anterior lens mass, among the population of cells fated to become anterior epithelium. TUNEL-positive cells were observed both at the anterior surface of the delaminating lens and deep to the surface (Supplementary Fig. S1B, <http://www.iovs.org/cgi/content/full/51/3/1540/DC1>) and were not concentrated

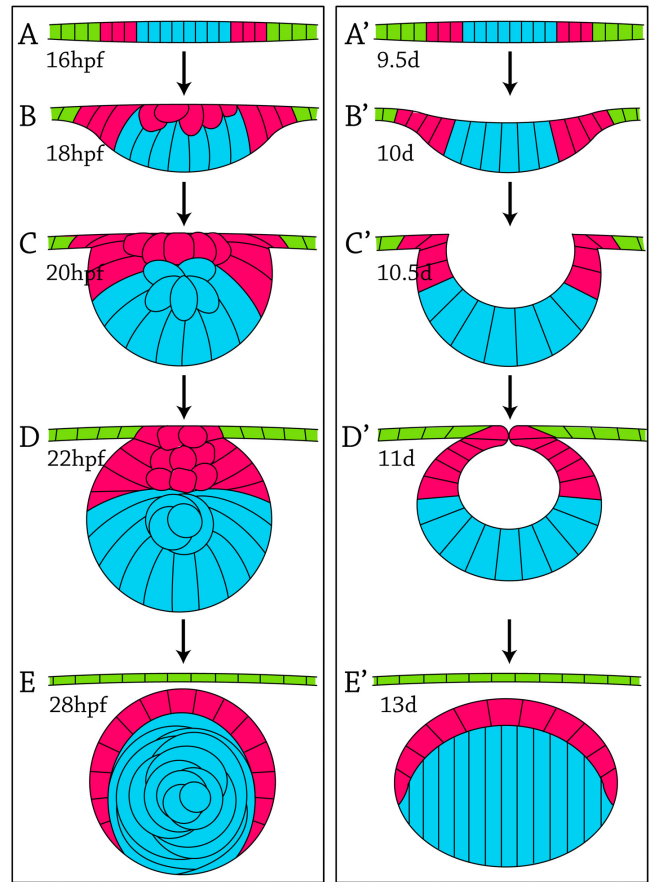


FIGURE 7. Comparison of lens development in the zebrafish (A-E) and mouse (A'-E') with color-coded cell-fate maps: primary fibers (*blue*), anterior lens epithelium (*pink*), and cornea (*green*). All cells in this diagram would be nucleated (not shown). Approximate ages are listed in hpf for the zebrafish and days (d) for the mouse.

at the point of separation between lens and cornea. TUNEL-positive cells were most abundant at approximately 25 to 26 hpf, after final delamination was complete. These results did not support the hypothesis that apoptosis was primarily associated with delamination. Instead, apoptosis might have been important in the reorganization of cells in the lens mass to form the anterior epithelium. In embryos aged 28 to 75 hpf, apoptotic cells were rarely

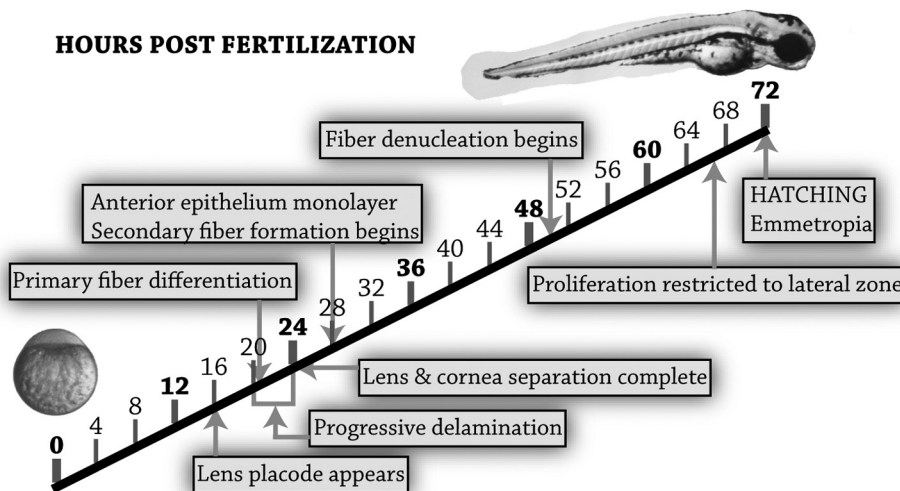


FIGURE 6. Time line of cellular differentiation events in the zebrafish lens from the zygote to 3 days after fertilization, when the lens became a functional optical element in the visual pathway.

observed in the lens and were occasionally seen in the retina or cornea (Fig. 4). Primary and secondary fiber cells undergoing nuclear breakdown during normal differentiation were not TUNEL positive.

Fiber Cell Maturation

To maximize lens transparency, fiber cells undergo a breakdown of nuclei, and all organelles large enough to scatter light disappear during elongation and maturation. In the zebrafish lens, all cells remained nucleated until approximately 50 hpf, when the cells at the very center of the embryonic lens nucleus no longer stained with DAPI (Fig. 4D). A spherical region of nonnucleated cells expanded in size until approximately 65 hpf (a few hours before hatching), after which time only the anterior epithelium and elongating fiber cells in the transition zone remained nucleated (Fig. 4F).

DISCUSSION

This report established a fate map for differentiating cells in the zebrafish lens using real-time live-embryo imaging. Immunohistochemistry was used to correlate cellular migration with proliferation, cell death, and differentiation during lens development from the placode to the functional optical element at hatching. Primary fiber cell differentiation and elongation began at 20 to 21 hpf in the posterior lens mass, as evidenced by the fiber cell-specific marker ZI-1, decreased BrdU staining, and live-cell morphology. After this stage, proliferation was restricted to cells fated to become anterior epithelium, which continued until approximately 68 hpf, when proliferation was restricted to a lateral proliferative zone, out of the optical path. Delamination was a progressive process from 20 to 24 hpf that did not include apoptosis as a primary mechanism for separation from the future cornea because apoptosis was not specific to the lens stalk. Apoptosis in the anterior lens cell mass continued for a few hours after final separation of the lens and cornea in cells fated to become anterior epithelium. Nuclear breakdown and fiber cell maturation began in the lens nucleus at approximately 50 hpf. All the major events in lens maturation to achieve a functional optical element in the visual pathway occurred before hatching at 72 hpf (Fig. 6). Despite the absence of a lens vesicle, cell differentiation during lens development was similar in the zebrafish and mammal.

Two-photon imaging of living zebrafish embryos with mosaic tomato red expression allowed individual lens cells to be tracked in real-time to determine cell fate during development. We observed two patterns of cell fate, one for primary fiber cells and another for epithelial cells, which are summarized and compared with the widely accepted (but unconfirmed) mammalian lens fate map in Figure 7. Cells in the zebrafish central lens placode (Fig. 7A, blue cells) migrated to the posterior lens mass (Figs. 7B, C) and elongated and differentiated as primary fiber cells (Figs. 7D, E). This pattern is consistent with models for development of the mammalian lens. Cells in the mammalian central lens placode (Fig. 7A', blue cells) moved to the posterior lens pit and lens vesicle (Figs. 7B'-D') and elongated to form primary fiber cells (Fig. 7E'). Cells in the zebrafish peripheral lens placode (Fig. 7A, pink cells) migrated to the anterior lens mass (Fig. 7C) and formed a single layer of anterior epithelium (Fig. 7E). Similarly, cells in the mammalian peripheral lens placode (Fig. 7A', pink cells) and composing the anterior lens vesicle (Fig. 7D') formed the anterior epithelium (Fig. 7E'). Thus, both zebrafish and mammalian cell fates can be predicted by position in the lens placode or anterior-posterior position in the lens mass/lens vesicle. The patterns of cell movement during development suggested that similar genetic mechanisms may control development in both the zebrafish and the mammalian lens.

The lack of a vesicle stage during zebrafish lens development has been described as a major difference in zebrafish and mammalian lens development. Although this obvious developmental difference may be important, it is not unique to the lens. Other important zebrafish tissues and organs also lack a vesicle stage or hollow cavity during development, including the neural "tube" (neural keel), optic "vesicle" (optic primordium), otic "vesicle," blastula, and gastrula stages, all of which develop as solid masses of cells.^{10,20-22} The fact that solid tissue development seems to be a theme throughout zebrafish development and yet zebrafish closely resemble mammalian development in other mechanisms suggests that the lack of a lens vesicle stage may not indicate a dramatically different mechanism of lens development.

Cell proliferation was examined in the zebrafish lens with the use of BrdU incorporation. Studies in the rodent and chick lens demonstrated proliferation throughout the lens placode and lens vesicle.²³ Primary fibers exited the cell cycle as elongation began.²⁴⁻²⁶ Proliferation in epithelial cells at the anterior pole of the rat lens (anterior to the adult proliferative zone) dropped dramatically over the first 2 postnatal weeks, which corresponds with eyelid opening at approximately 17 days.²⁷⁻²⁹ The pattern of proliferation in the mammalian and chick lens is similar to that observed in the zebrafish lens. All vertebrates studied exhibited proliferation throughout the developing lens until primary fibers began elongation, at which point fibers exited the cell cycle. Elongation of primary fibers in the zebrafish lens was observed in real-time during live two-photon imaging and was found to coincide temporally with decreased BrdU incorporation and ZI-1 expression. In both mammals and zebrafish, proliferation of the entire anterior epithelium continued until hatching in fish or eyelid opening in mice. At that stage, proliferation was restricted to a lateral zone out of the optical path. Decreased proliferation in the central epithelium corresponded with the onset of functional vision in both species. These studies demonstrated similarities between vertebrates during lens development.

Apoptosis occurs in the mammalian lens at the approximate time that the lens vesicle pinches off from the surface ectoderm. In mammals, cell death was observed at the edges of the shallow lens pit, between the medial and lateral one-third of cells that make up the lens cup, in the degenerating lens stalk during separation of the lens vesicle, and in the anterior half of the lens vesicle, all regions fated to contribute to the anterior epithelium.^{25,30-33} Different hypotheses have been postulated regarding the role of cell death in the separating lens vesicle, from "loosening" of the placode to assisting in bending of the flat placode into a vesicle, to a mechanical role in pinching off the lens vesicle, to a lack of "impetus for differentiation" which leads to degeneration. Rapidly shifting junctional complexes have been observed during separation of the lens vesicle in chick, and cadherins are vital for normal separation of the mouse lens vesicle.^{33,34}

In the zebrafish lens, apoptosis might have played a minor role in the final separation of the lens mass from the surface ectoderm because occasional apoptotic cells were detected at the anterior surface of the lens mass at 23 hpf. However, delamination is a progressive process resembling epithelial-mesenchymal transition, occurring from approximately 20 to 24 hpf,¹ and apoptosis did not occur in the lens before 23 hpf. Apoptosis was not a primary mechanism of separation of lens and cornea in the zebrafish lens. In the absence of apoptosis, delamination in the zebrafish lens may be the result of shifting junctions and adhesion complexes like those observed in the chick and mouse lens vesicle. Actin, focal adhesions, and cadherins can be expected to participate in the mechanisms of separation in response to transcription and growth factors. Apoptosis continued in the zebrafish lens until approximately 26 hpf, 2 hours after separation of the lens mass from the surface ectoderm, in the cells of the

developing anterior epithelium. The functional role of apoptosis in these cells remains elusive and may be related to differentiation of the anterior epithelium into a single layer of cells. More studies are needed on this subject.

TUNEL labeling was not detected in zebrafish fiber cells undergoing nuclear breakdown during terminal differentiation. Other experiments have demonstrated TUNEL staining in differentiating fiber cells, including in the adult zebrafish lens.^{12,35,36} Because TUNEL-positive cells were detected in the embryonic retina, cornea, and lens epithelium, it is uncertain whether the absence of staining in differentiating embryonic fibers is a functional difference in zebrafish embryonic fiber maturation.

In summary, our results using live-embryo imaging determined that the cells in the periphery of the lens placode become lens epithelium, and cells in the center of the lens placode become primary fibers, establishing the similarity between teleost and mammalian lens development. The results confirm the expectations of previous reports on the similarities between zebrafish and mouse lens development despite the lack of a hollow lens vesicle stage in zebrafish.^{9,12,37,38} The conservation of cell fates suggests that genetic mechanisms are conserved during vertebrate lens development. Future studies using live-cell markers expressed in the developing lens of the living zebrafish are expected to advance our understanding of the molecular and genetic basis for organogenesis that occurs during human development.

Acknowledgments

The authors thank Rachel O. Wong for her advice, without which this work could not have been performed; David White for his technical expertise with zebrafish care and maintenance; and Hidayat Djajadi for his work on immunohistochemistry.

References

- Greiling TM, Clark JL. Early lens development in the zebrafish: a three-dimensional time-lapse analysis. *Dev Dyn*. 2009;238:2254–2265.
- Lang RA. Pathways regulating lens induction in the mouse. *Int J Dev Biol*. 2004;48:783–791.
- Lovicu FJ, Robinson ML. *Development of the Ocular Lens*. Cambridge, UK: Cambridge University Press; 2004.
- Schoenwolf GC, Bleyl SB, Brauer PR, Francis-West PH. *Larsen's Human Embryology*. Philadelphia: Churchill Livingstone/Elsevier; 2009.
- Vihhtelic TS. Teleost lens development and degeneration. *Int Rev Cell Mol Biol*. 2008;269:341–373.
- Iyengar L, Wang Q, Rasko JE, McAvoy JW, Lovicu FJ. Duration of ERK1/2 phosphorylation induced by FGF or ocular media determines lens cell fate. *Differentiation*. 2007;75:662–668.
- Chamberlain CG, McAvoy JW, Richardson NA. The effects of insulin and basic fibroblast growth factor on fibre differentiation in rat lens epithelial explants. *Growth Factors*. 1991;4:183–188.
- de Jongh RU, Lovicu FJ, Overbeek PA, et al. Requirement for TGFbeta receptor signaling during terminal lens fiber differentiation. *Development*. 2001;128:3995–4010.
- Soules KA, Link BA. Morphogenesis of the anterior segment in the zebrafish eye. *BMC Dev Biol*. 2005;5:12.
- Schmitt EA, Dowling JE. Early eye morphogenesis in the zebrafish, *Brachydanio rerio*. *J Comp Neurol*. 1994;344:532–542.
- Easter SS Jr, Nicola GN. The development of vision in the zebrafish (*Danio rerio*). *Dev Biol*. 1996;180:646–663.
- Dahm R, Schonthaler HB, Soehn AS, van Marle J, Vrensen GF. Development and adult morphology of the eye lens in the zebrafish. *Exp Eye Res*. 2007;85:74–89.
- Godinho L, Mumm JS, Williams PR, et al. Targeting of amacrine cell neurites to appropriate synaptic laminae in the developing zebrafish retina. *Development*. 2005;132:5069–5079.
- Kay JN, Roeser T, Mumm JS, et al. Transient requirement for ganglion cells during assembly of retinal synaptic layers. *Development*. 2004;131:1331–1342.
- Lohmann C, Mumm JS, Morgan J, et al. Imaging the developing retina. In: Yuste R, Konnerth A, eds. *Imaging in Neuroscience and Development*. Cold Spring Harbor, NY: Cold Spring Harbor Laboratory Press; 2005:171–183.
- Shi X, Luo Y, Howley S, et al. Zebrafish foxe3: roles in ocular lens morphogenesis through interaction with pitx3. *Mech Dev*. 2006;123:761–782.
- Link BA, Kainz PM, Ryou T, Dowling JE. The perplexed and confused mutations affect distinct stages during the transition from proliferating to post-mitotic cells within the zebrafish retina. *Dev Biol*. 2001;236:436–453.
- Cole LK, Ross LS. Apoptosis in the developing zebrafish embryo. *Dev Biol*. 2001;240:123–142.
- Biehlermaier O, Neuhauss SC, Kohler K. Onset and time course of apoptosis in the developing zebrafish retina. *Cell Tissue Res*. 2001;306:199–207.
- Kimmel CB, Ballard WW, Kimmel SR, Ullmann B, Schilling TF. Stages of embryonic development of the zebrafish. *Dev Dyn*. 1995;203:253–310.
- Haddon C, Lewis J. Early ear development in the embryo of the zebrafish, *Danio rerio*. *J Comp Neurol*. 1996;365:113–128.
- Lowery LA, Sive H. Strategies of vertebrate neurulation and a re-evaluation of teleost neural tube formation. *Mech Dev*. 2004;121:1189–1197.
- Modak SP, Morris G, Yamada T. DNA synthesis and mitotic activity during early development of chick lens. *Dev Biol*. 1968;17:544–561.
- McAvoy JW. Cell division, cell elongation and the co-ordination of crystallin gene expression during lens morphogenesis in the rat. *J Embryol Exp Morphol*. 1978;45:271–281.
- Schook P. Morphogenetic movements during the early development of the chick eye: a light microscopic and spatial reconstructive study. *Acta Morphol Neerl Scand*. 1980;18:1–30.
- Lovicu FJ, McAvoy JW. Spatial and temporal expression of p57(KIP2) during murine lens development. *Mech Dev*. 1999;86:165–169.
- Hanna C, O'Brien JE. Cell production and migration in the epithelial layer of the lens. *Arch Ophthalmol*. 1961;66:103–107.
- Mikulicich AG, Young RW. Cell proliferation and displacement in the lens epithelium of young rats injected with tritiated thymidine. *Invest Ophthalmol*. 1963;2:344–354.
- McAvoy JW, McDonald J. Proliferation of lens epithelial explants in culture increases with age of donor rat. *Curr Eye Res*. 1984;3:1151–1153.
- Aso S, Tashiro M, Baba R, Sawaki M, Noda S, Fujita M. Apoptosis in the lensanlage of the heritable lens aplastic mouse (lap mouse). *Teratology*. 1998;58:44–53.
- Mohamed YH, Amemiya T. Apoptosis and lens vesicle development. *Eur J Ophthalmol*. 2003;13:1–10.
- Bozanic D, Tafra R, Saraga-Babic M. Role of apoptosis and mitosis during human eye development. *Eur J Cell Biol*. 2003;82:421–429.
- Schook P. Morphogenetic movements during the early development of the chick eye: an ultrastructural and spatial study. C. Obliteration of the lens stalk lumen and separation of the lens vesicle from the surface ectoderm. *Acta Morphol Neerl Scand*. 1980;18:195–201.
- Pontoriero GF, Smith AN, Miller LA, Radice GL, West-Mays JA, Lang RA. Co-operative roles for E-cadherin and N-cadherin during lens vesicle separation and lens epithelial cell survival. *Dev Biol*. 2009;326:403–417.
- Bassnett S, Mataic D. Chromatin degradation in differentiating fiber cells of the eye lens. *J Cell Biol*. 1997;137:37–49.
- Bassnett S. Fiber cell denucleation in the primate lens. *Invest Ophthalmol Vis Sci*. 1997;38:1678–1687.
- Gross JM, Perkins BD, Amsterdam A, et al. Identification of zebrafish insertional mutants with defects in visual system development and function. *Genetics*. 2005;170:245–261.
- Posner M, Hawke M, Lacava C, Prince CJ, Bellanco NR, Corbin RW. A proteome map of the zebrafish (*Danio rerio*) lens reveals similarities between zebrafish and mammalian crystallin expression. *Mol Vis*. 2008;14:806–814.